

Spatial Profile of Deposition Rate of a-Si:H Films in Multi-Hollow Discharge Plasma Chemical Vapor Deposition

W. M. Nakamura, D. Shimokawa, H. Miyahara, K. Koga, and M. Shiratani

Department of Electronics, Kyushu University, Motoooka 744, Fukuoka 819-0395, Japan

Fax: 81-92-802-3734, e-mail: w.nakamura@plasma.ed.kyushu-u.ac.jp

A high defect density of hydrogenated amorphous silicon (a-Si:H) is one of the main reasons for a low efficiency of a-Si:H solar cells. An increase in defect density of conventional a-Si:H is brought about by light exposure (light induced degradation). In the present work we employed a multi-hollow discharge plasma chemical vapor deposition (CVD) method to control the stability of a-Si:H films. The films deposited in the downstream region and in the upstream region near the discharges of the multi-hollow discharge plasma CVD reactor show light induced degradation, while ones in the upstream region far from the discharges show no degradation. The deposition rate of the species generated in the discharges decreases with increasing the distance between the substrate and the discharge, according to their surface reaction probabilities and diffusion velocities.

Key words: light induced degradation, multi-hollow discharge plasma CVD, a-Si:H, cluster, dangling bond

1. INTRODUCTION

Light exposure increases a defect density in a-Si:H leading to a reduction of qualities of devices based on a-Si:H (e.g. efficiency of solar cells) [1,2]. Hence, such light induced degradation of a-Si:H films has been an important issue to enhance the efficiency of a-Si:H solar cells. Some studies indicate that a-Si:H films with a low hydrogen content associated with Si-H₂ bond (C_{SiH₂}) show high stability against light exposure [3,4], even though the mechanism which leads to light induced degradation remains unclear. Therefore, the species responsible for the formation of Si-H₂ bonds should be identified in order to reduce their deposition into films. SiH₃ radicals, high order silane related radicals (HOS radicals), and amorphous silicon nanoparticles (clusters) are generated in SiH₄ discharges during a-Si:H film deposition. SiH₃ radicals are the main precursor of the film deposition, HOS radicals are molecules of Si_mH_n (m<4, n ≤ 2m + 2) in a size range below 0.5 nm, while clusters are nanoparticles in a size range between 0.5 nm and 10 nm. Both, HOS radicals and clusters, can be incorporated into films during deposition, and then they could be associated with the Si-H₂ bond formation. In our previous work, we developed a cluster-suppressed plasma CVD method, which combines the reduction of gas flow stagnation regions with the exertion of thermophoretic and gas viscous forces on clusters to prevent their deposition. By using this method we found out that C_{SiH₂} decreases with decreasing the volume fraction of clusters incorporated into films [5,6], and we obtained films with C_{SiH₂} < 3×10⁻² at.% [7]. The films without incorporating clusters were highly stable against light exposure. Moreover, incorporation of HOS radicals into the films is not relevant to the formation of Si-H₂ bonds [8]. However, the contribution of clusters between 0.5nm and 1nm in size to the light induced degradation still unknown.

To increase the deposition rate of the cluster-suppressed plasma CVD method we develop a multi-hollow discharge plasma CVD method [9]. In this

method, the cluster suppression is made by setting a gas flow velocity high enough to drive the clusters toward the downstream region. Since the diffusion velocity of the clusters is much lower than the diffusion velocity SiH₃ radicals, we can then obtain films without incorporation of clusters in the upstream region. The a-Si:H films deposited in the upstream region show high stability against light exposure.

Recently, we studied the dependence between the distance from the discharge region and the deposition rate obtained in the upstream region of the multi-hollow discharge plasma CVD. Moreover, we calculated the expected deposition rate of the different species using a simulation. We present these experimental and simulated results in this paper. These results will help us to control the stability of the a-Si:H films and to identify the minimum size of clusters which contribute to the light induced degradation.

2. EXPERIMENTAL

The multi-hollow discharge plasma CVD reactor had three electrodes, each with 24 holes of 5mm in diameter and placed 2mm apart in a stainless steel tube of 75mm in inner diameter. Figure 1 shows the experimental setup. Pure SiH₄ was supplied at 40sccm from the bottom of the reactor throughout the electrodes, pumped by a molecular drag pump (ALCATEL MDP5030). The total pressure was 200 Pa. The temperature of the reactor was kept isothermal at 250°C to avoid thermophoretic force on clusters due to thermal gradient. The discharge frequency was 60 MHz, and the discharge power was 45 W. The discharges were sustained in the holes where SiH₃, HOS radicals and clusters were generated. Figure 2 shows the top view of discharges.

We placed a glass substrate in the upstream region parallel to the gas flow. After deposition the sample was separated in 5 columns and 10 rows as shown in Fig.3, and we measured the thickness of each piece along the axial axis z and compared the results between different

columns c. The film thickness was measured with an optical transmission spectroscop (JASCO V-570).

3. RESULTS AND DISCUSSION

3.1 Stability of films

The films deposited in the downstream region and in the upstream region near the discharges of the multi-hollow discharge plasma CVD reactor show light induced degradation, while ones in the upstream region far from the discharges show no degradation.

3.2 Dependence of deposition rate on distance from discharge

Figure 4 shows the deposition rate in the upstream region as a distance from the discharge region. The results show that the deposition rate decreases exponentially with the distance, and this exponential decrease is nearly independent on the radial position.

Figure 5 shows the deposition rate along the radius as a parameter of the distance from the discharge region. The results show that the decrease in the deposition rate along

the radius is also nearly independent on a position in the axial axis.

These two results indicate that we can treat the dependence of the deposition rate on the distance along axial and radius axis independently.

3.3 Theoretical modeling

Here we modeled the particle density n of SiH₃ radicals, which is the main precursor of the film deposition, in the reactor as a first step to understand the dependence of the deposition rate on the distance from the discharge to the substrate for each precursor. This first model takes into account a cylindrical reactor in which the SiH₃ radicals are generated in a planar source $S(z)$ located at the origin of $z=0$, and diffuse along the radius and the axial axis with loss to the walls (see Fig.3). We started with the diffusion equation:

$$\frac{\partial n}{\partial t} - D\nabla^2 n = S(z) - kn^2, \tag{1}$$

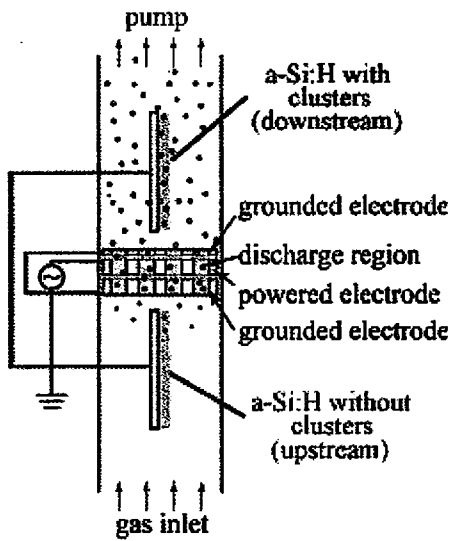


Fig. 1. Multi-hollow discharge plasma CVD reactor.

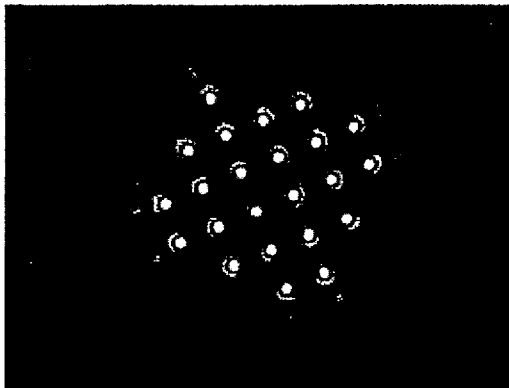


Fig. 2. Top view of discharges.

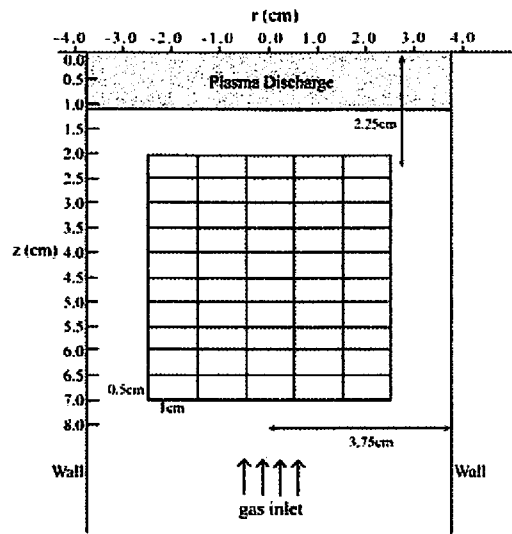


Fig. 3. Schematic of substrate in upstream region of reactor.

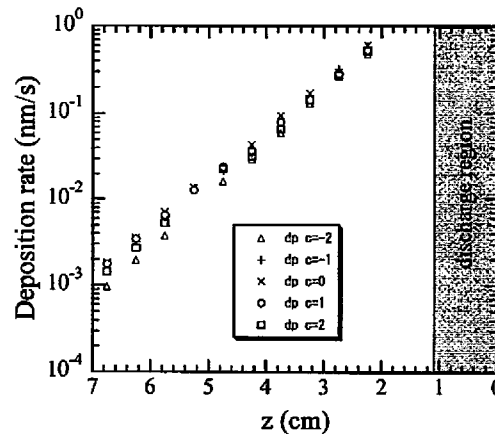


Fig. 4. Dependence of deposition rate of multi-hollow discharge plasma CVD method on distance from discharge region.

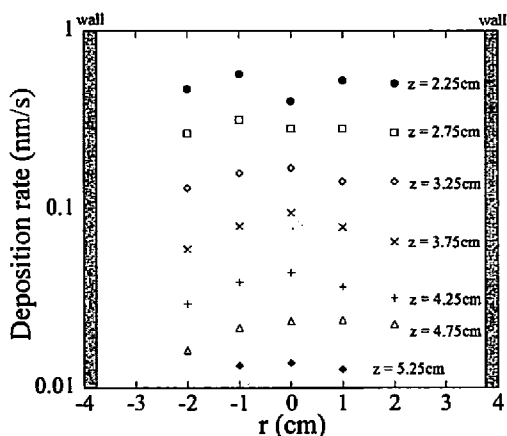


Fig. 5. Deposition rate along radius as a parameter of distance from discharge region.

where D is the diffusion coefficient, the source is $S(z) = S\delta(z)$, and k is the rate constant for biradical recombination. The term kn^2 was neglected because it was much smaller than $D\nabla^2 n$ and $S(z)$ under our conditions. Firstly we solved the equation with the method of separation of variables for $z \neq 0$, considering the steady state ($\partial n / \partial t = 0$) and n without any angular dependence.

The obtained solution is

$$n(r, z) = n_0 J_0\left(\frac{r}{\Lambda}\right) \exp\left(-\frac{z}{\Lambda}\right), \quad (2)$$

where Λ and n_0 are constants. The solution of the radial part is a Bessel function of order zero $J_0(r/\Lambda)$, and the axial part is represented by an exponential decrease along z axis.

Here we considered that the wall does not absorb all the particles that hit on. The diffusion length Λ is then

$$\Lambda^2 = \Lambda_0^2 + l_0 \lambda, \quad (3)$$

where: $\Lambda_0 = R/2.405$ [10]. We consider that the reactor has a semi-infinite axial length from the source.

$$l_0 = \frac{V_{reactor}}{A_{reactor}} \rightarrow \lim_{h \rightarrow \infty} l_0 = \frac{R}{2}, \quad (4)$$

and the linear extrapolation length is

$$\lambda = \frac{4 \cdot D \cdot (1 - \beta/2)}{v_{th} \cdot \beta}, \quad (5)$$

where β is the surface reaction probability of SiH_3 radicals at the walls, and v_{th} is the thermal speed.

Figure 6 shows the theoretical results obtained with the model. The β was obtained from the analysis of the

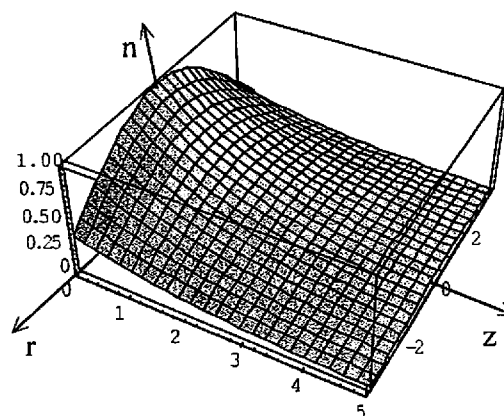


Fig.6. Simulation result for SiH_3 density profile.

radial profile of the experimental deposition rate, which indicates a value around 0.04. This value is very low compared to the accepted literature value around 0.28 [10].

Comparing the results of the theoretical model with the experimental data we computed two values of β , one for the axial part and another for the radial part, though the model indicate that they should be the same. For the radial part $\beta \approx 0.04$ and for the axial part $\beta > 1$, which suggest that another parameters should be taken into account. Such difference between the model and the experimental results may be due to the presence of the substrate which increases the loss. Another possibility is that our real sources are the electrode holes instead of the supposed planar source.

The results also showed the dependence of the deposition rate on the diffusion coefficient, which indicates that the deposition of different species can be controlled by changing the position of the substrate for a given deposition condition. Hence, combining this information with the film's stability against light soaking may indicate which specie is responsible for the light

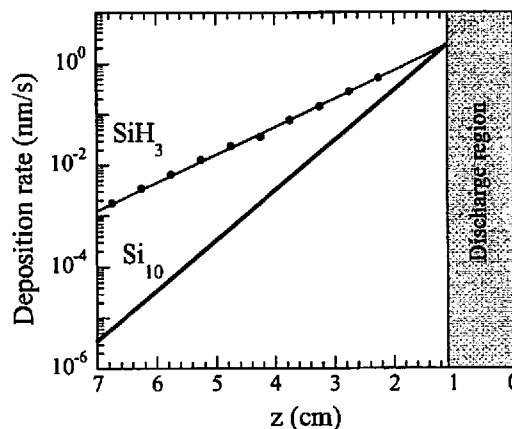


Fig. 7. Dependence of deposition rate for different species on distance z from discharge region.

induced degradation of the film.

Since the substrate itself can be considered as a wall on which precursors are lost, we calculated an effective radius of the chamber to take the substrate influence into account. This result allowed us to calculate the expected density decrease for other species. Figure 7 shows the theoretical results of the deposition rate for Si_{10} species (calculated with $\beta = 1$) together with the experimental ones (solid circles) for SiH_3 deduced from the deposition rate.

These results show that the deposition rate of Si_{10} decreases faster than the SiH_3 even in this simple model without considering the influence of the gas flow on species.

4. CONCLUSIONS

The experimental deposition rate in the upstream region decreases exponentially with the distance to the discharge region along axial axis in the multi-hollow discharge plasma CVD method. As the deposition rate depends on the diffusion velocities of the species, it is possible to control the spatial density profile of each precursor deposition. The theoretical model for the density profile must be improved to handle the influence of other parameters such as loss on the substrate.

5. ACKNOWLEDGMENTS

This work was partly supported by the Industrial Technology Development Organization (NEDO). The authors would like to acknowledge the assistance of

Messrs T. Kinoshita and H. Matsuzaki.

6. REFERENCES

1. D. L. Staebler and C. R. Wronsky, *Appl. Phys. Lett.*, **31**, 292 (1979).
2. R. E. I. Schropp and M. Zeman, *Amorphous and Microcrystalline Silicon Solar Cells*, Kluwer Academic, Boston, p. 47 (1998).
3. T. Nishimoto, M. Takai, H. Miyahara, M. Kondo, and A. Matsuda, *J. Non-Cryst. Solids*, **299**, 1116 (2002).
4. S. Shimizu, H. Miyahara, M. Shimosawa, and M. Kondo, A. Matsuda, *Proceedings of the 3rd World Conference on Photovoltaic Energy Conversion*, 5P-A9-03 (2003).
5. K. Koga, N. Kaguchi, M. Shiratani, and Y. Watanabe, *J. Vac. Sci. Technol.*, **A22**, 1536-39 (2004).
6. K. Koga, M. Kai, M. Shiratani, Y. Watanabe, N. Shikatani, *Jpn. J. Appl. Phys.*, **41**, L168 (2002).
7. Y. Watanabe, A. Harikai, K. Koga, and M. Shiratani, *Pure Appl. Chem.*, **74**, 483 (2002).
8. M. Shiratani, K. Koga, N. Kaguchi, K. Bando, and Y. Watanabe, *Thin Solid Films*, 506-507, p17-21 (2006).
9. K. Koga, T. Inoue, K. Bando, S. Iwashita, M. Shiratani, and Y. Watanabe, *Jpn. J. Appl. Phys.*, **44**, L1430 (2005).
10. J. Perrin, M. Shiratani, P. Kae-Nune, H. Videlot, J. Jolly, and J. Guillon, *J. Vac. Sci. Technol. A*, **16**, 1, p278-289 (1998).

(Received January 23, 2007; Accepted March 7, 2007)